IEEE Photonics Journal
An IEEE Photonics Society Publication

Actively Q-Switched Tm:YAP Laser Constructed Using an Electro-Optic Periodically Poled Lithium Niobate Bragg Modulator

Volume 12, Number 5, October 2020

Shou-Tai Lin
Zhao-Ren Qiu
Cheng-Po Chen

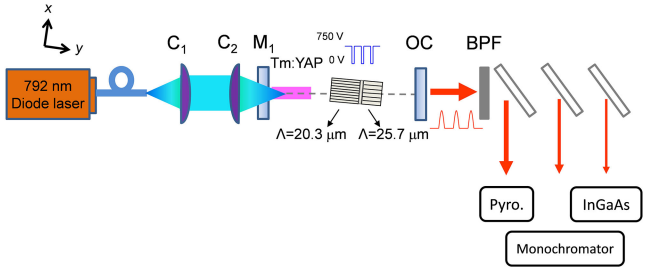

DOI: 10.1109/JPHOT.2020.3020074

Actively Q-Switched Tm:YAP Laser Constructed Using an Electro-Optic Periodically Poled Lithium Niobate Bragg Modulator

Shou-Tai Lin, Zhao-Ren Qiu, and Cheng-Po Chen

Department of Photonics, Feng Chia University, Taichung 40724, Taiwan

DOI:10.1109/JPHOT.2020.3020074

Manuscript received August 13, 2020; accepted August 24, 2020. Date of publication August 31, 2020; date of current version September 14, 2020. This work was supported in part by the Ministry of Science and Technology (MOST), Taiwan (MOST 108-2221-E-035-073), and in part by the National Chung-Shan Institute of Science and Technology (NCSIST), Taiwan. Corresponding author: Shou-Tai Lin (e-mail: stailin@fcu.edu.tw).

Abstract: We present an EO Q-switched Tm:YAP laser constructed with a periodically poled Mg-doped congruent lithium niobate (PPMgCLN) Bragg modulator. A 2-mm-thick PPMgCLN modulator was adopted, and the internal stress generated in the electric poling process was released by annealing. The peak stress-induced refractive index variance for e-wave was deduced to be 2.29×10^{-5} at 1064 nm. When the absorbed pump power and repetition rate were 13.4 W and 1 kHz, respectively, the laser had a Q-switched pulse energy of 2 mJ, a pulse duration of 60 ns, and a peak power of 33.3 kW. By varying the reflection of the output coupler, output wavelengths of between approximately 1985 and approximately 1940 nm can be selected, making this laser a potential tool for pumping mid-IR sources and biomedical applications.

Index Terms: Diode-pumped lasers, Q-switched lasers.

1. Introduction

Two-micrometer lasers have been widely adopted for several applications including eye-safe light detection and ranging, plastic welding, wind speed measurement, and ambient gas detection [1]. Due to a high water absorption peak of 1940 nm in such lasers, one promising application is in medicine, where they offer considerable potential for precise surgery with minimal blood flow [2]. For applications in the mid-infrared (IR) range, Q-switched 2-μm lasers can be used to pump a ZGP optical parametric oscillator [3]. To prevent absorption loss and thermal issues in ZGP crystals, a pump laser wavelength longer than 2 μm is preferable [4]. An atmospheric window of 2–2.4 μm is used for remote gas sensing, including for carbon monoxide, hydrogen fluoride, and methane [5]. Among available laser gain medium, thulium-doped yttrium aluminum perovskite (Tm:YAP) crystal has been widely employed to generate tunable laser sources between 1.87 and 2.04 μm in range due to their high absorption band (nearly 800 nm) that can be pumped directly by an economic diode laser system [6]. Inherent crystal birefringence is also benefited to generate linear output polarization and process further nonlinear frequency conversion. Several Q-switching devices are typically adopted in pulsed 2-μm lasers, including active acousto-optic modulators (AOMs) [7], electro-optic modulators (EOMs) [8], and passive saturable absorbers (SAs) [9].

Compared with passive Q-switching (PQS), the advantages of active Q-switching are released cavity design, controlled Q-switch timing, and stable pulse energy. Moreover, SA materials, such as Cr^{2+}:ZnS and Cr^{2+}:ZnSe, can be hampered by damage and thermal instability, which can cause an increase in pulse duration and a nonrecoverable decline in PQS laser performance [9]. Compared with AOMs, EOMs have advantages with regard to their energy efficiency and compact size; an additional cooling scheme is not required. Electro-optic periodically poled lithium niobate Bragg modulators (EPBMs) have been demonstrated to have low applied voltage and to be insensitive to temperature [10]. Cascaded different grating periods of EPBMs have been demonstrated to have broad operation bandwidth and multiple wavelength outputs [11]. Furthermore, engineerable grating vectors can monolithically integrate EOMs and nonlinear frequency converters [12]. Due to the low damage threshold (100 MW/cm^2 at 1064 nm) [13] and limited thickness, $\sim$1 mm, of periodically poled congruent lithium niobate (PPCLN), the practical applications of EPBM were restricted and only $\sim$200 μJ pulse energy was demonstrated in Nd:YVO_4 laser [10]. Periodically poled magnesium-doped congruent lithium niobate (PPMgCLN) has a thickness of up to 10 mm [14], giving it potential application for producing a high-energy electro-optic (EO) Q-switched laser. In this paper, we demonstrate an EO Q-switched Tm:YAP laser using an EPBM with pulse energy greater than 2 mJ. Compared with a previous report [10], a 10-fold improvement was achieved.

2. Device Characterization

When a z-component electric field E_z is applied on PPMgCLN, the refractive index differences induced by the EO effect for extraordinary (z polarization) and ordinary (x or y polarization) waves with different domain orientations can be given by the following equations:

$$\Delta n_e = \mp \frac{n_e^3 \gamma_{33} E_z}{2}, \tag{1}$$

$$\Delta n_0 = \mp \frac{n_0^3 \gamma_{13} E_z}{2}, \tag{2}$$

where n_e and n_0 are extraordinary and ordinary refractive indices, respectively, and γ_{33} and γ_{13} are the Pockels coefficients for extraordinary and ordinary waves, respectively. Because the γ_{33} value of an EPBM is more than three times larger than that of γ_{13} [15], alignment of laser polarization to the z-axis can be conducted using a lower half-wave voltage. Therefore, we fixed the laser polarization in the z-direction for the following discussion. The sign $\mp$ represents the induced refractive index change in the positive and negative domain orientations. To efficiently process the diffraction, the incident angle must match the Bragg incident angle, $\theta_{B,m} = \sin^{-1}\left[m\lambda_0/(2n_e\Lambda)\right]$, where m is the diffraction order, λ_0 is the laser wavelength in a vacuum, and Λ is the grating period. When the first order diffraction ($m = 1$) and sinusoidal refractive index variation are considered, the half-wave voltage of an EPBM can be expressed by $V_\pi = \frac{\pi}{4} \frac{\lambda_0}{\gamma_{33} n_e^3} \frac{t}{L}$ [10], where t is the thickness of an EPBM in the z-axis, and L is the Bragg grating length in the y-axis, as shown in Fig. 1. The high-order Fourier components of the square-function PPMgCLN grating become significant at voltages higher than V_π [10].

To achieve a moderate V_π, a 2-mm-thick PPMgCLN with a grating period of 20.3 μm was adopted in the EPBM. The $\pm$z surfaces of the EPBM were coated with NiCr electrodes for applying electric field. A z-polarized continuous-wave (cw) laser at 1064 nm with $M^2 < 1.3$ was used to measure the diffraction efficiency. The laser beam waist radius was controlled to approximately 120 μm at the center of the EPBM. Two types of EPBM, namely EPBM1 and EPBM2, were used for comparison, as shown in Table 1. Fig. 2 shows 0th-order transmittance when the laser incident angle was matched with the first order diffraction (Bragg incident angle: $\sim$0.7°). The triangular and square dots show that EPBM1 and EPBM2 were composed of PPCLN and PPMgCLN, respectively. V_π was measured at approximately 230 V/mm for both EPBMs, and diffraction loss of approximately 50% was identified at the bottom of both transmission curves. This slightly higher value for V_π can be attributed to an imperfect poling process. The diffraction loss was related to the incident

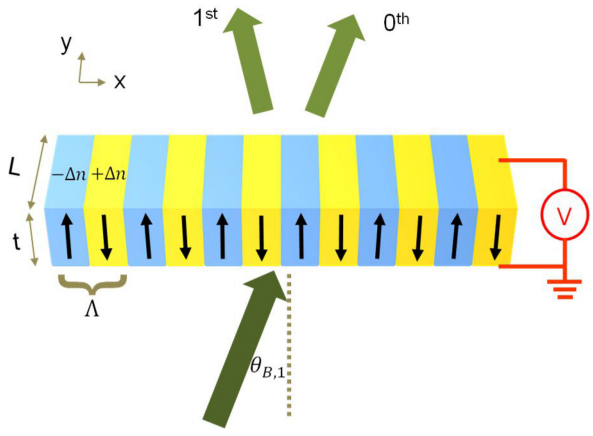

Fig. 1. An EO Bragg modulator is constructed using PPMgCLN, and the applied voltage is in the z direction.

TABLE 1
Dimensions and V_π of EPBM1 and EPBM2

	Dimensions (X × Y × Z/mm^3)	Calculated V_π (V/mm)	Measured V_π (V/mm)
EPBM1 (PPCLN)	10 x 17 x 0.78	175	230
EPBM2 (PPMgCLN)	10 x 15 x 2	199	235

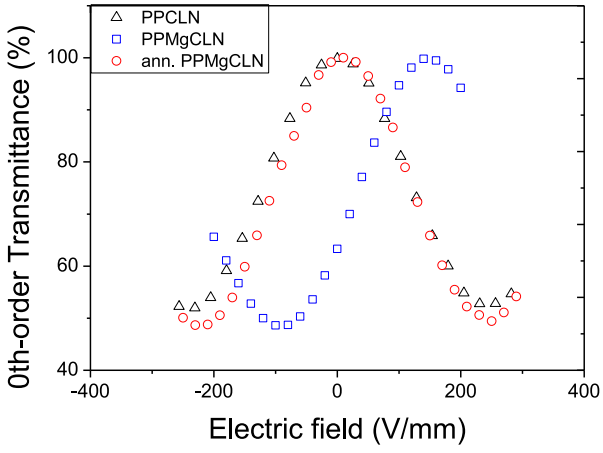

Fig. 2. Measured 0th-order transmittance versus applied voltage for three EPBMs.

beam waist radius. The smaller beam waist radius corresponding to a large angular spectrum had poor diffraction loss because some energy was not matched by the Bragg condition [10]. Although a 2-mm-thick PPMgCLN crystal provides a large aperture and reduces the difficulty of alignment, the high stress-induced refractive index changed [11], [16] between adjacent poling domains, leading to peak transmittance shifting approximately 300 V from zero-point voltage. From (1), the peak stress-induced refractive index variance for e-wave was calculated to be 2.29×10^{-5} for $\gamma_{33} = 30.3\ pm/V$ and $n_e = 2.147$ at 1064 nm. To reduce stress, an annealing process was performed at 550°C for 24 h [17]. The circular dots in Fig. 2 show peak transmittance at 0 V,

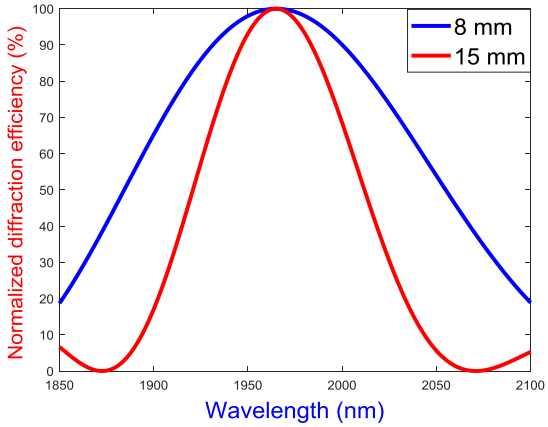

Fig. 3. Calculated EO Bragg modulator diffraction efficiency versus wavelength. The incident Bragg angle is fixed at 1.297° (angle matched at 1.965 μm), and the applied voltage is V_π.

and V_π remained at approximately 230 V. Thus, internal stress was successfully reduced by the annealing process, and poling quality was unaffected. Because the gain bandwidth of Tm:YAP is more than 167 nm [6], the diffraction bandwidth of the EPBM should also be considered. Adopting the plane wave model, the diffraction efficiency at mismatched Δk can be expressed as follows [18]:

$$\eta(\Delta k) = \frac{|A_2(L)|^2}{|A_1(0)|^2} = \frac{|\kappa|^2}{|\kappa|^2 + \left(\frac{1}{2}\Delta k\right)^2} \sin^2\left\{\left[|\kappa|^2 + \left(\frac{1}{2}\Delta k\right)^2\right]^{1/2} L\right\} \tag{3}$$

where A_1 and A_2 are the incident and diffracted electric field, respectively, $\kappa = \frac{2\gamma_{33} n_e^3}{\lambda_0} \frac{V}{t}$ is the coupling coefficient, and Δk is the wave vector mismatched in the y direction. Fig. 3 shows the calculated diffraction efficiency for two different EPBM lengths when the incident Bragg angle is fixed at 1.297° (angle matched at 1.965 μm) and the applied voltage is V_π. The diffraction bandwidths (FWHMs) of EPBMs 8 and 15 mm in length are estimated to be 170 and 90 nm, respectively. Because the length of EPBM2 (15 mm) provides inadequate diffraction bandwidth for the whole gain spectrum of Tm:YAP, we adopted another currently obtainable EPBM that has an 8-mm-long Bragg grating and a diffraction bandwidth of 170 nm.

3. Q-switched Tm:YAP Laser

Fig. 4 presents the experimental configuration of a Q-switched Tm:YAP laser constructed with an EPBM device. We adopted an *a*-cut, 9-mm-long, 4 at.% Tm–doped YAP crystal with an aperture of 3 $\times$ 3 mm^2 as the gain medium, which had peak absorption at approximately 795 nm. To prevent thermal cracking issues, a diode laser of approximately 792 nm was used, and diode power of over 80% was absorbed in a single pass configuration. The gain medium was coated with antireflection (AR) coating at approximately 800 nm (R $<$ 5%), and 1850–2050 nm (R $<$ 1%) on both incident surfaces. To dissipate heat, the Tm:YAP crystal was wrapped with indium foil and kept in a copper block with water cooling at 15°C. The core radius of the pump diode laser was 100 μm and refocused into the gain medium through a set of 1 to 2 coupling lenses. The laser cavity was constructed in a flat–flat configuration. The input coupler M_1 was coated with highly reflective coating (R $>$ 99.8%) at 1850–2050 nm and high-transmission coating (T $>$ 95%) at approximately 800 nm. The EO Q-switched crystal was composed of cascaded PPMgCLN gratings (EPBM3/EPBM4) with dimensions of 10 mm (width in x) $\times$ 15.5 mm (length in y) $\times$ 2 mm (thickness in z). The grating period of EPBM3 was 20.3 μm, and the dimensions were 10 mm (width in x) $\times$

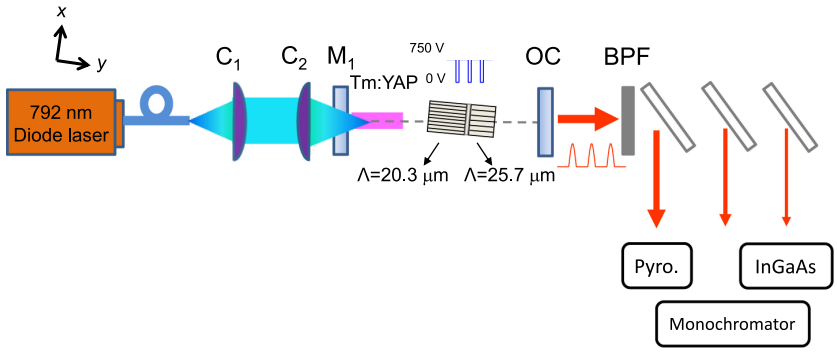

Fig. 4. Experimental configuration of an EO Q-switched Tm:YAP laser constructed using a cascaded EPBM.

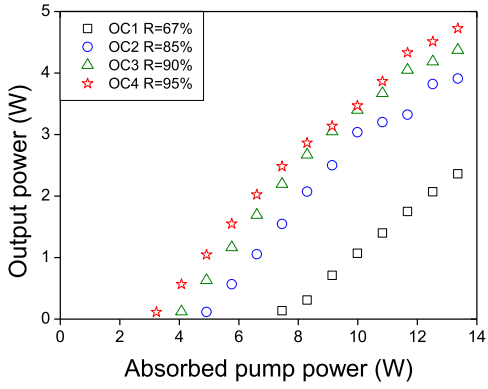

Fig. 5. Experimental results for the cw Tm:YAP laser versus different OCs.

8 mm (length in y). The grating period of EPBM4 was 25.7 μm, and the dimensions were 10 mm (width in x) $\times$ 5.5 mm (length in y). To reduce stress-induced refractive index variance, the cascaded EPBM was annealed after the poling process. The input faces of the cascaded EPBM were then optically polished and had AR coating applied at 1850–2050 nm (R $<$ 2%). To utilize the EO effect, the NiCr electrodes were coated on $\pm$z surfaces. Total cavity length was maintained around 5.5 cm. A 2 μm bandpass filter (BPF, FWHM $=$ 500 nm) was used to block the residual diode power and prevent errors in measurement. A voltage pulser with a 750-V amplitude was adopted to maintain a low Q (high-loss) state in the cavity and store energy in the upper state of the Tm:YAP laser. The Q-switched pulse was generated in a high Q state (low loss) during the range of a 1-μs pulse width at zero voltage. Although this EPBM had a cascaded grating (20.3/25.7 μm), the Bragg angles at approximately 2 μm for the two grating periods were 1.3° and 1.05°, respectively. Using (3), the theoretical diffraction efficiency reached 60% at 750 V when the incident angle was fixed at 1.3°. Because of the large mismatched incident angle of EPBM4 (25.7 μm), the contribution of diffraction efficiency was negligible. The cascaded EPBM can be treated as a single-grating 8-mm EPBM. A pyroelectric detector was used to measure the pulse energy, and pulse duration was recorded by a biased InGaAs detector (900–2600 nm, 17 ns rise time) with a 500 MHz bandwidth oscilloscope. The laser wavelength was measured by a grating-based scanning monochromator with 0.5 nm resolution and was averaged 100 times at each data point.

4. Experimental Results and Discussion

When the cascaded EPBM was matched with the Bragg incident angle ($\sim$1.3°), the maximum output pulse energy was found. Before recording the Q-switched process, we turned off the voltage

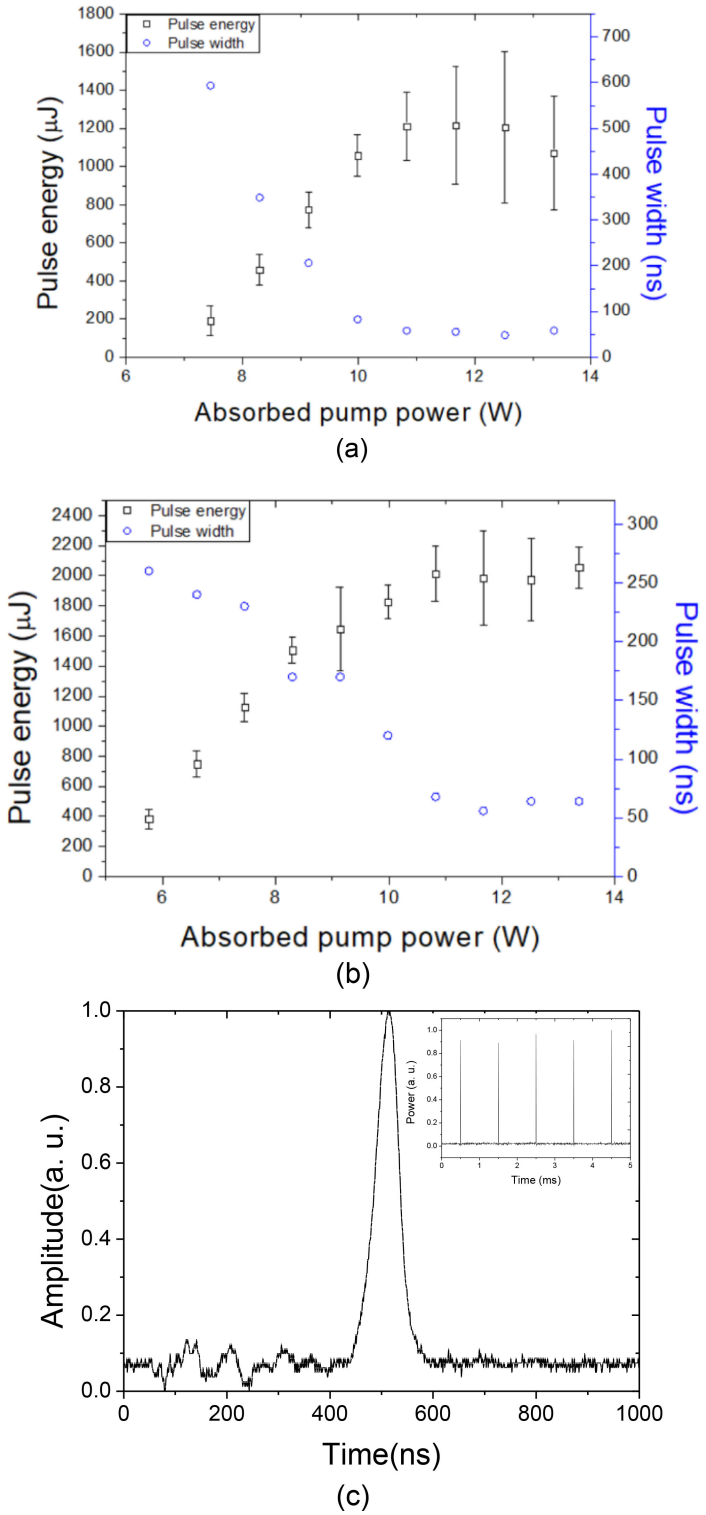

Fig. 6. Measured output energy, and pulse duration at a repetition rate of 1 kHz. (a) OC1 (R = 67%). (b) OC2 (R = 85%). (c) typical pulse waveform when the absorbed pump power was higher than 10 W.

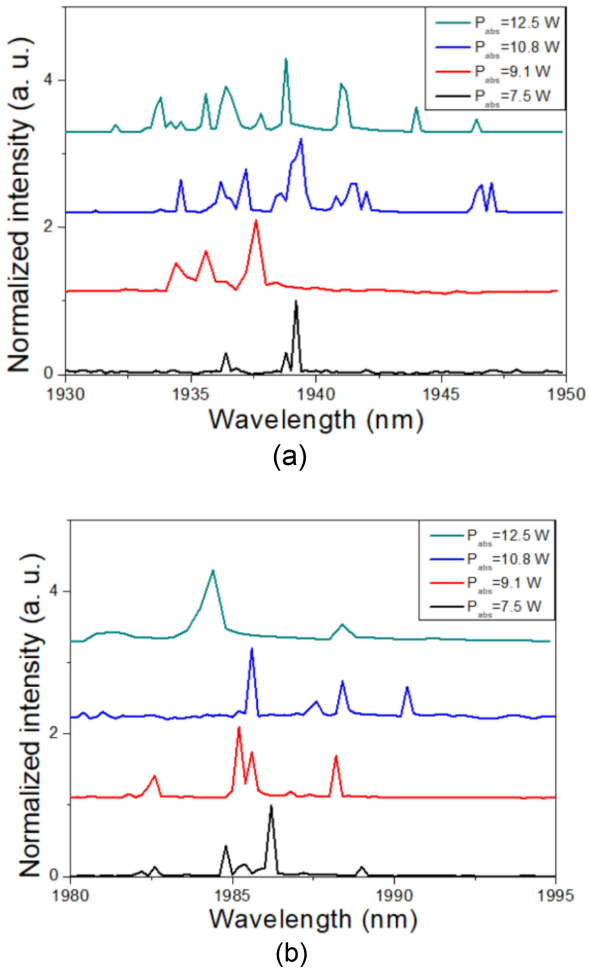

Fig. 7. Measured output spectra at different absorbed pump powers. (a) OC1 (R = 67%). (b) OC2 (R = 85%).

pulser and characterized the cw Tm:YAP laser under four output couplers (OC 1–4), as shown in Fig. 5. The measured reflectance values of the OCs are in the range of 1850–2050 nm with 1% variation. A thermal detector was used to record average power. When OC4 (R = 95%) was adopted, an output power greater than 4.5 W was reached at an absorbed pump power of 13.4 W, with optical slope efficiency of 46% and optical conversion efficiency of 35%. The recorded slope efficiency was lower than that in a published report [9], but the imperfect AR coating of the EPBM may explain this result. To prevent optical damage to the EPBM, the Q-switched repetition rates were set higher than 1 kHz, and only OC1 (R = 67%) and OC2 (R = 85%) were used in the following experiment. Fig. 6 shows the measured output pulse energy, pulse duration and pulse waveforms. To measure energy instability, the measured pulse energy and standard deviation were averaged and analyzed over 2 min. The measured pulse duration was averaged from 1024 pulses. When the absorbed pump power was 13.4 W, the measured output pulse energy was 1.1 and 2 mJ for OC1 and OC2, respectively. The measured pulse duration was approximately 60 ns, as shown in Fig. 6(c), corresponding to peak power of approximately 18 kW and 33 kW. Because the diffraction efficiency of the EPBM was sensitive to the beam radius [10], the strong thermal lensing and reduced resonated beam radius limited loss holding ability. When the absorbed pump power was greater than 11 W, the measured pulse energy was saturated and cw lasing output was observed. To remedy insufficient loss modulation in the high pump power regime, applying

higher voltage to the EPBM would increase loss modulation. However, currently available pulser voltage is limited at 750 V. With regard to output performance, OC2 had higher pulse energy and lower energy fluctuation than OC1. The averaged energy fluctuations were 11% and 22.8% in OC2 and OC1, respectively. The measured pulse durations decreased to approximately 60 ns when the absorbed diode power was greater than 10 W. A simple linear cavity composed of two cavity mirrors helped to reduce cavity length and produce a short pulse duration. The measured output spectra at different absorbed pump powers are shown in Fig. 7. The wavelength was shifted from approximately 1985 nm to approximately 1940 nm when the output coupler was replaced from OC2 to OC1, consistent with the model of reabsorption loss and polarization effects [19]. Without an intracavity wavelength-selective element, such as a birefringent plate or etalon, multi-longitudinal modes of oscillation were expected. Energy instability caused by mode competition and lower over-pumping ratio (pumping/cavity threshold) can explain the high energy fluctuation in OC1 [20], [21]. To further characterize the wavelength-shift issue, we measured the cw output spectra of the four OCs. When the reflection of the output coupler was higher than 85% (OC 2–4), the measured output wavelengths were in the range of 1985–1990 nm; a longer wavelength was observed in the output coupler with relatively high reflection, which matched the model of reabsorption loss [19].

5. Summary

In conclusion, we describe the performance of an EO Q-switched Tm:YAP laser constructed with a cascaded PPMgCLN Bragg modulator. The high stress-induced refractive index variance between adjacent poling domains in EPBMs was reduced through annealing. With absorbed pump power of 13.4 W, a repetition rate of 1 kHz, and R of 85% in the output coupler, a pulse energy of 2 mJ, a pulse duration of 60 ns, and a peak power of 33.3 kW were achieved. Without any intracavity wavelength-selective element, the output wavelengths can be switched between approximately 1985 and approximately 1940 nm when OCs with R of 85% and 67% are used. Both unique output wavelengths are promising developments for pumping mid-IR sources and biomedical applications.

References

[1] K. Scholle, S. Lamrini, P. Koopmann, and P. Fuhrberg, "2 μm laser sources and their possible applications," *Frontiers in Guided Wave Optics and Optoelectronics*. Rijeka, Croatia: InTech, 2010.

[2] G. E. Tontini *et al.*, "Ex vivo experimental study on the Thulium laser system: new horizons for interventional endoscopy (with videos)," *Endoscopy Int. Open*, vol. 5, no. 6, pp. E410–E415, Mar. 2017.

[3] B. Cole *et al.*, "Compact and efficient mid-IR OPO source pumped by a passively Q-switched Tm:YAP laser," *Opt. Lett.*, vol. 43, no. 5, pp. 1099–1102, Mar. 2018.

[4] L. Wang *et al.*, "Mid-infrared ZGP-OPO with a high optical-to-optical conversion efficiency of 75.7%," *Opt. Express*, vol. 25, no. 4, pp. 3373–3380, Feb. 2017.

[5] L. Guillemot *et al.*, "Continuous-wave Tm:$YAlO_3$ laser at $\sim$2.3 μm," *Opt. Lett.*, vol. 44, no. 20, pp. 5077–5080, Oct. 2019.

[6] H. Jelínková, P. Koranda, J. Šulc, M. Nemec, P. Cerný, and J. Pašta, "Diode pumped Tm:YAP laser for eye micro-surgery," in *Proc. SPIE*, vol. 6871, 2008, Art. no. 68712N.

[7] S. S. Cai *et al.*, "Room-temperature cw and pulsed operation of a diode-end-pumped Tm:YAP laser," *Appl. Phys. B*, vol. 90, no. 1, pp. 133–136, Nov. 2008.

[8] L. Guo *et al.*, "Diode-wing-pumped electro-optically Q-switched 2 μm laser with pulse energy scaling over ten millijoules," *Opt. Express*, vol. 26, no. 13, pp. 17731–17738, Jun. 2018.

[9] B. Cole and L. Goldberg, "Highly efficient passively Q-switched Tm:YAP laser using a Cr:ZnS saturable absorber," *Opt. Lett.*, vol. 42, no. 12, pp. 2259–2262, Jun. 2017.

[10] S. T. Lin, G. W. Chang, Y. Y. Lin, Y. C. Huang, A. C. Chiang, and Y. H. Chen, "Monolithically integrated laser Bragg Q-switch and wavelength converter in a PPLN crystal," *Opt. Express*, vol. 15, no. 25, pp. 17093–17098, Dec. 2007.

[11] S. T. Lin, S. Y. Hsu, Y. Y. Lin, and Y. Y. Lin, "Selectable dual-wavelength actively Q-switched laser by monolithic electro-optic periodically poled lithium niobate Bragg modulator," *IEEE Photon. J.*, vol. 5, no. 5, Oct. 2013, Art. no. 1501507.

[12] W. K. Chang *et al.*, "Two-dimensional PPLN for simultaneous laser Q-switching and optical parametric oscillation in a Nd:YVO_4 laser," *Opt. Express*, vol. 19, no. 24, pp. 23643–23651, Nov. 2011.

[13] P. Belden, D. Chen, and F. D. Teodoro, "Watt-level, gigahertz-linewidth difference-frequency generation in PPLN pumped by an nanosecond-pulse fiber laser source," *Opt. Lett.*, vol. 40, no. 6, pp. 958–961, Mar. 2015.

[14] H. Ishizuki and T. Taira, "Half-joule output optical-parametric oscillation by using 10-mm-thick periodically poled Mg-doped congruent $LiNbO_3$," *Opt. Express*, vol. 20, no. 18, pp. 20002–20010, Aug. 2012.

[15] A. Yariv and P. Yeh, *Optical Waves in Crystals*. New York, NY, USA: Wiley, 1984, pp. 230–234.
[16] Y. Chen, H. Zhan, and B. Zhou, "Refractive index modulation in periodically poled MgO-doped congruent $LiNbO_3$," *Appl. Phys. Lett.*, vol. 93, no. 22, Dec. 2008, Art. no. 222902.
[17] M. Paturzoa, D. Alfieri, S. Grilli, P. Ferraro, and P. D. Natale, "Investigation of electric internal field in congruent $LiNbO_3$ by electro-optic effect," *Appl. Phys. Lett.*, vol. 85, no. 23, Dec. 2004, Art. no. 5652.
[18] R. W. Boyd, *Nonlinear Optics*. New York, NY, USA: Elsevier, 2003, pp. 393–402.
[19] R. C. Stoneman and L. Esterowiz, "Efficient 1.94-μm Tm:YALO laser," *IEEE J. Sel. Topics Quantum Electron.*, vol. 1, no. 1, pp. 78–81, Apr. 1995.
[20] J. Dong and K. I. Ueda, "Longitudinal-mode competition induced instabilities of Cr^{4+}, Nd^{3+}:$Y_3Al_5O_{12}$ self-Q-switched two-mode laser," *Appl. Phys. Lett.*, vol. 87, no. 15, Oct. 2005, Art. no. 151102.
[21] J. Brooks, G. M. Bonner, A. J. Kemp, and D. J. M. Stothard, "Stability of Q-switched 2 μm lasers," *OSA Continuum*, vol. 3, no. 3, pp. 568–579, Mar. 2020.